Physics and Imaging in Radiation Oncology 18 (2021) 26–33

Contents lists available at ScienceDirect

Physics and Imaging in Radiation Oncology

journal homepage: www.sciencedirect.com/journal/physics-and-imaging-in-radiation-oncology

Multi-parametric magnetic resonance imaging assessment of whole tumour heterogeneity for chemoradiotherapy response prediction in rectal cancer

Trang Thanh Pham [a,b,*], Gary Liney [a], Karen Wong [b], Christopher Henderson [c], Robba Rai [b], Petra L. Graham [e], Nira Borok [f], Minh Xuan Truong [f], Mark Lee [b], Joo-Shik Shin [c,d], Malcolm Hudson [g], Michael B. Barton [a]

[a] *Ingham Institute for Applied Medical Research, South West Sydney Clinical School, Faculty of Medicine, University of New South Wales, Sydney, PO Box 3151, Liverpool, NSW 2170, Australia*
[b] *Department of Radiation Oncology, Liverpool Cancer Therapy Centre, Liverpool Hospital, Sydney, Locked Bag 7103, Liverpool BC, NSW 1871, Australia*
[c] *Department of Anatomical Pathology, Liverpool Hospital, Sydney, Locked Bag 7103, Liverpool BC, NSW, 1871, Australia*
[d] *School of Medicine, Western Sydney University, Sydney, Locked Bag 1797, Penrith, NSW 2751, Australia*
[e] *Centre for Economic Impacts of Genomic Medicine, Macquarie Business School and Department of Mathematics and Statistics, Faculty of Science and Engineering, Macquarie University, Sydney, Macquarie University, NSW 2109, Australia*
[f] *Department of Radiology, Liverpool Hospital, Sydney, Locked Bag 7103, Liverpool BC, NSW 1871, Australia*
[g] *NHMRC Clinical Trials Centre, Sydney, Locked Bag 77, Camperdown, NSW 1450, Australia*

A B S T R A C T

Background and purpose: Prediction of chemoradiotherapy response (CRT) in locally advanced rectal cancer would enable stratification of management. The purpose was to prospectively evaluate multi-parametric magnetic resonance imaging (MRI) assessment of tumour heterogeneity combining diffusion weighted imaging (DWI) and dynamic contrast enhanced (DCE) MRI for the prediction of CRT response in locally advanced rectal cancer.
Materials and methods: Patients with Stage II or III rectal adenocarcinoma undergoing neoadjuvant CRT and surgery underwent MRI (DWI and DCE) before, during (week 3), and after CRT (1 week before surgery). Patients with histopathology tumour regression grade (TRG) 0–1 were classified as responders, and TRG 2–3 were classified as non-responders. A whole tumour voxel-wise technique was used to produce apparent diffusion coefficient (ADC) and K^{trans} (Tofts model) histograms derived from DWI and DCE-MRI, respectively. Logistic regression was used to predict response status for ADC and K^{trans} quantiles.
Results: Thirty-three patients were included in this analysis; 16 responders, and 17 non-responders. On heterogeneity analysis, odds of being a responder were significantly higher after CRT (before surgery) for higher ADC 75th ($p = 0.049$) and ADC 90th ($p = 0.034$) percentile values. The K^{trans} quantiles were lower in non-responders than responders before and during CRT, and higher after CRT although no significant association with response status was observed ($p \geq 0.10$).
Conclusions: DWI-MRI after CRT (before surgery) incorporating a histogram analysis of whole tumour heterogeneity was predictive of CRT response in patients with locally advanced rectal cancer. DCE-MRI did not add value in response prediction.
Clinical trial registration: Australian New Zealand Clinical Trials Registry (ANZCTR) number ACTRN12616001690448.

1. Introduction

The addition of pre-operative radiotherapy to primary surgery for treatment of locally advanced rectal cancer has decreased locoregional recurrence rates [1–5], and increased overall survival [2,6]. Neo-adjuvant chemo-radiotherapy (CRT) has the advantage of tumour downstaging, with a pathologic complete response (pCR) achieved in 15–27% of patients [7]. There is risk of significant treatment morbidity and over a third of patients will have a permanent colostomy as a result of surgery [1,8]. Tumour responses vary following CRT [9] and there is currently no accurate method of predicting CRT response. Current predictive models require pathological staging, making them unsuitable for use as a pre-treatment decision tool [10,11].

Early imaging prediction of CRT response would enable a personalised treatment approach to improve therapeutic response and avoid treatment morbidity. Prediction of a complete response to CRT prior to surgery would enable a 'watch-and-wait' approach, avoiding the morbidity of surgery. Prediction of non-responders prior to CRT could

* Corresponding author at: Locked Bag 7103, Liverpool BC, NSW 1871, Australia.
E-mail addresses: Trang.Pham@health.nsw.gov.au (T.T. Pham), Gary.Liney@health.nsw.gov.au (G. Liney), Karen.Wong4@health.nsw.gov.au (K. Wong), Christopher.Henderson@health.nsw.gov.au (C. Henderson), Robba.Rai@health.nsw.gov.au (R. Rai), Petra.Graham@mq.edu.au (P.L. Graham), Nira.Borok@health.nsw.gov.au (N. Borok), Minh.Truong@health.nsw.gov.au (M.X. Truong), Mark.Lee2@health.nsw.gov.au (M. Lee), j.shin@westernsydney.edu.au (J.-S. Shin), Malcolm.Hudson@mq.edu.au (M. Hudson), Michael.Barton@health.nsw.gov.au (M.B. Barton).

https://doi.org/10.1016/j.phro.2021.03.003
Received 9 November 2020; Received in revised form 3 February 2021; Accepted 18 March 2021
Available online 13 April 2021

allow these patients to proceed directly to surgery thereby avoiding toxicity of futile treatment. If non-responders are detected after CRT (prior to surgery), a radiotherapy boost could be added in order to improve complete response rate. Functional magnetic resonance imaging (MRI) biomarkers have greater potential compared to standard T2-weighted sequences for therapeutic response prediction in locally advanced rectal cancer [12,13]. Studies have demonstrated apparent diffusion coefficient (ADC) derived from diffusion weighted imaging (DWI) to be useful for the prediction of CRT response [14–16]. The ability of ADC to differentiate viable tumour (low ADC) from necrosis (high ADC) makes it a useful biomarker to monitor early effects of radiotherapy [17]. Dynamic contrast enhanced (DCE) MRI studies in rectal cancer have shown correlation of DCE parameters such as K^{trans} with tumour angiogenesis, as indicated by micro-vessel density and vascular endothelial growth factor, and tumour downstaging [18–22]. However, most published MRI response prediction studies in rectal cancer report single summary parameters such as the mean value from either diffusion or perfusion MRI and do not provide information on tumour heterogeneity.

Tumours are biologically heterogeneous, and multi-parametric MRI combining DWI and DCE would provide a more comprehensive biological assessment of cellularity and perfusion. A whole tumour assessment such as histogram analysis [23], would capture information on tumour heterogeneity that may affect therapeutic response. There are limited studies in multi-parametric MRI in the prediction of CRT response in locally advanced rectal cancer [24,25]. There are currently no published prospective studies assessing DWI and DCE-MRI with a whole tumour heterogeneity analysis for the prediction of therapeutic response in locally advanced rectal cancer.

The aim of this study was to prospectively evaluate multi-parametric MRI whole tumour heterogeneity analysis using DWI and DCE-MRI at 3.0 T performed before, during and after CRT for therapeutic response prediction in locally advanced rectal cancer.

2. Materials and methods

2.1. Patients

This prospective study was approved by the local Human Research and Ethics Committee. Informed consent was obtained from all patients. Patients with Stage II or III rectal adenocarcinoma undergoing neoadjuvant CRT followed by primary surgery were eligible. The inclusion criteria were (i) age >18 years, (ii) locally advanced rectal adenocarcinoma Stage II or III (T3 – T4 and/or N1 – 2), without distant metastases staged as per tumour node metastatsis (TNM) American Joint Committee on Cancer (AJCC) 7th edition [26], (iii) neoadjuvant CRT and primary surgery. The exclusion criteria were: (i) prior malignancy, (ii) active inflammatory bowel disease, (iii) contraindication to MRI. Patients with mucinous adenocarcinomas confirmed on subsequent histopathology were excluded from the analysis due to these tumours having predominately mucin and therefore different MRI characteristics to non-mucinous adenocarcinomas. All patients received standard treatment consisting of neoadjuvant CRT (radiotherapy to pelvis 45 Gy/25#, boosting tumour to 50.4 Gy/28#, 3D-conformal, IMRT or VMAT, concurrent infusional 5-fluorouracil (1575 mg/m^2 over 7 days) or oral capecitabine (825 mg/m^2 bd), followed by surgery (total mesorectal excision, low/ultra-low anterior resection or abdomino-perineal resection) 6–12 weeks after completion of CRT. Of 39 patients recruited, 6 had Stage IIA, 1 had Stage IIIA, 25 had Stage IIIB, and 7 patients had Stage IIIC disease at diagnosis. All 39 patients had MRI before CRT, 37 patients had MRI during CRT (2 refused MRI), and 32 patients had MRI after CRT (7 refused MRI). Of the 39 patients, 2 patients were unable to undergo DCE-MRI due to renal contraindication to gadolinium contrast. Two patients refused surgery; of these 1 was lost to follow-up and excluded from analysis. Five patients with mucinous histopathology were excluded from this analysis, leaving 33 patients with non-mucinous adenocarcinoma in the analysis. Three DCE-MRIs at a single time-point were excluded from analysis due to poor image quality from technical issues.

2.2. MRI technique and analysis

Patients underwent MRI at 3.0 T consisting of DWI (RESOLVE, b-values 50 and 800 s/mm^2) and DCE (pre-contrast VIBE with flip angles 2° and 15° followed by gadoversetamide (Optimark) (0.1 mM/kg) injection and 60 phases using TWIST, 5 s temporal resolution) with butylscopolamine (Busocapan) to halt rectal peristalsis at 3 time-points: (i) Before CRT, (ii) during CRT (week 3 of CRT), and (iii) after CRT (within 1 week prior to surgery). Further details on MRI technique are in the study protocol [27] and Appendix 1. ADC maps and calculated b = 1400 mm/s^2 images were produced as part of protocol. Rigid body manual registration of flip-angle images to dynamic images was performed in 3D (Siemens version 40.1). Flip angle 2° and 15° images were used to calculate native T1. Tissue4D (Siemens version 1.0) was used to produce K^{trans} maps by first pre-selecting an appropriate arterial input function, scaled by dose, based on chi-squared goodness of fit, and using a two-compartment Tofts model. ADC (derived from DWI) and K^{trans} (derived from DCE) parameter maps were exported in DICOM format and registered to T2-w axial orthogonal images in OncoTreat (works-in-progress, Siemens version 3.1.1). Semi-automated segmentation was used to define the region of interest (ROI) from the entire hyper-intense tumour on the b-value 1400 mm/s^2 images. One observer with sub-specialisation in gastrointestinal malignancies performed all segmentations. A voxel-by-voxel technique was used to produce colour-coded maps and histograms of ADC and K^{trans}, and combined scatterplots for each time-point. The raw voxel-wise data was exported from OncoTreat WIP for statistical analysis.

2.3. Histopathology

Two pathologists with gastrointestinal sub-specialisation examined each case and reached a consensus on tumour regression grade (TRG). Specimen examination followed the guidelines in the Royal College of Pathologists of Australasia Structured Reporting Protocol for Colorectal Cancer [28]. The entire original tumour site was embedded for microscopic assessment. TRG was recorded using the modified classification of Ryan et al [29] in the AJCC Cancer Staging Manual, 7th Edition [26] as follows:

TRG 0 (complete response) – no viable cancer cells

TRG 1 (moderate response) – single cells or small groups of cancer cells

TRG 2 (minimal response) – residual cancer outgrown by fibrosis

TRG 3 (poor response) – minimal or no tumour kill; extensive residual cancer.

Patients with TRG 0–1 were categorised as ‘responders’ and those with TRG 2–3 were categorised as ‘non-responders’ to CRT. Histology type was categorised as adenocarcinoma, mucinous adenocarcinoma. Tumours with >50% mucin were classified as mucinous adenocarcinoma as per WHO definition.

2.4. Statistical analysis

Analyses were performed using R version 4.0.2. Whole tumour voxel-wise raw data was used for analysis. In the case of K^{trans}, transformation of the ROI values (after first excluding voxels with K^{trans} of 0) using the cube-root (symmetrising) transformation was undertaken. A continuous variable analysis was performed. Whole tumour ADC and K^{trans} distributions were produced for each patient, and histogram quantiles (10th, 25th, 50th, 75th, 90th), skewness (measure of asymmetry of the distribution [23]) and kurtosis (sharpness of the peak and shape of the distribution [23]) were extracted from ADC and K^{trans} distributions in order to determine if the quantile statistics differed between groups by

response status or changed time. Tumour heterogeneity was assessed by using objective cut-points defined by quantiles. The mean of each quantile, skewness and kurtosis was summarised by response status and time point.

Linear mixed-effects models were used to analyse temporal change in medians of ADC and K^{trans} with a random intercept to control for the repeated measurements on each patient over time. Dunnet multiple comparison with control (before CRT) tests were used to determine the mean difference from before to during CRT, and from before to after CRT for the whole cohort. Mixed-effects models utilise all available data to produce unbiased effect estimates, even in the presence of missing data, provided the missing values can be assumed to be missing at random.

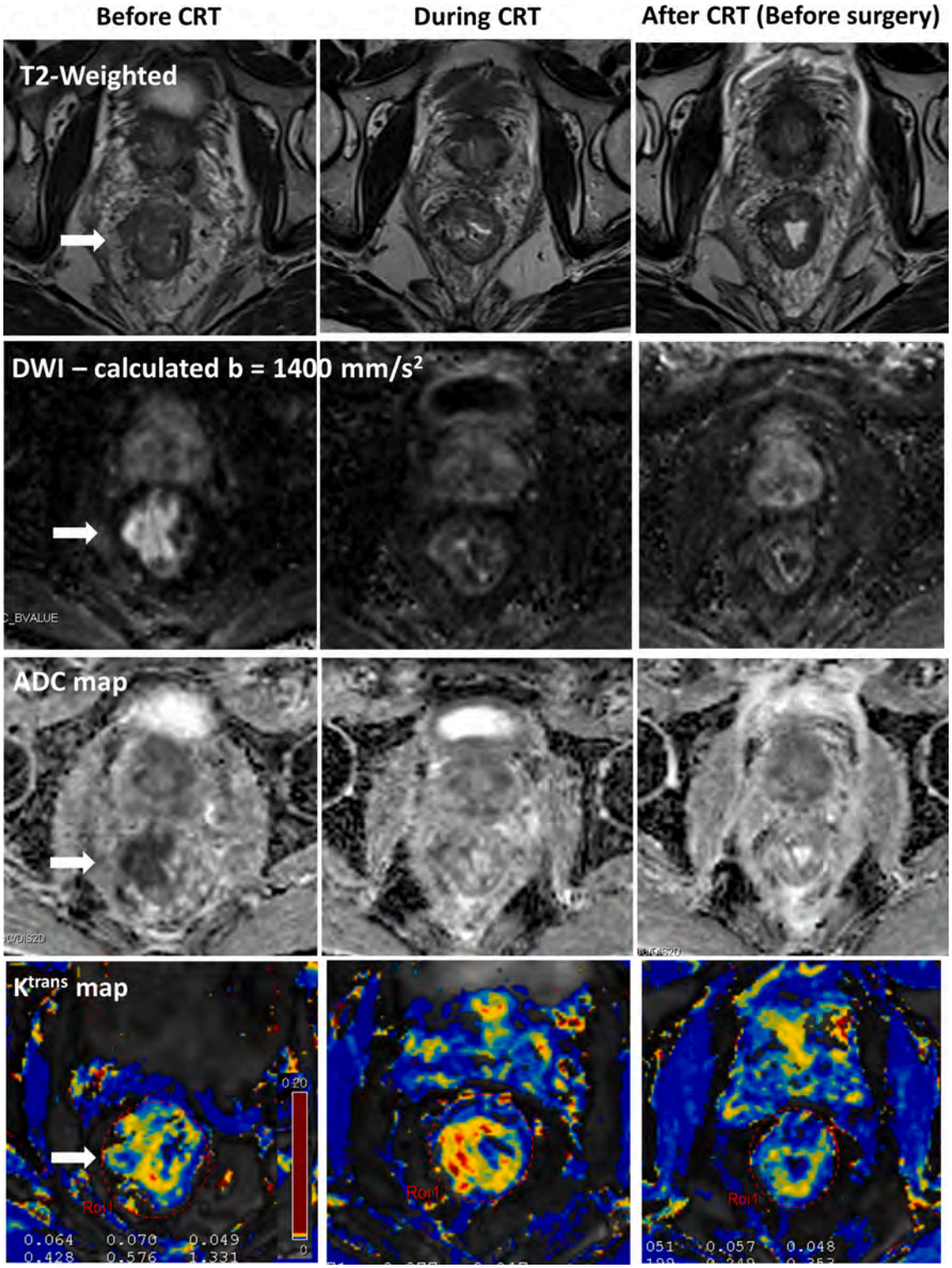

Fig. 1. Multi-parametric MRI at 3 time-points for a responder (TRG 0, pathologic complete response). The arrow indicates the rectal tumour. Tumour response during and after CRT was seen more clearly on the DWI and ADC map than the T2-weighted images. The K^{trans} maps showed the tumour had low perfusion at all time-points.

Univariate logistic regression was performed to investigate the odds ratio (OR) (ie. odds of a being a responder versus non-responder) for each of the ADC and K^{trans} histogram parameters 10th, 25th, 75th and 90th quantiles, skewness, and kurtosis by time-point. While adopting mixed-effects logistic models were of interest here, convergence issues precluded their use. As such analysis by separate time point was necessary. Area under the receiver operating curve (AUC) was calculated for each model and presented with 95% bootstrap confidence intervals. AUC close to 0.5 imply no discrimination ability of the predictor while values close to 1 imply outstanding discrimination. P-values < 0.05 were considered statistically significant.

3. Results

Three patients had pCR TRG 0 (9%), 12 had TRG 1 (36%), 14 had TRG 2 (42%), and 3 had TRG 3 (9%). One patient (3%) who refused surgery had a clinical complete response on colonoscopy and biopsy performed at 18 months, which was considered as a surrogate endpoint for pCR and classified as TRG 0. Sixteen patients were classified as responders (TRG 0–1), and 17 were classified as non-responders (TRG 2 – 3). The median time from completion of CRT to surgery was 64 days (range 40–119).

Representative MR images and the corresponding ADC and K^{trans} maps, histograms, and multi-parametric scatterplots for the whole tumour for a responder (TRG 0, pathologic complete response) are shown in Figs. 1 and 2, respectively, and for a non-responder (TRG 2, minimal response) are shown in Figs. 3 and 4, respectively. The representative DWI ADC histograms showed that the magnitude of shift in ADC voxels to higher values over time, indicating a reduction in tumour cellularity in response to CRT, was greater in the responder than non-responder. The DCE K^{trans} histograms showed that perfusion was greater after CRT in the non-responder indicating increased tumour perfusion.

For all patients with non-mucinous adenocarcinoma, a temporal change in ADC was found, but not for K^{trans} (Table 1). There was a significant mean increase in all ADC quantiles (10th, 25th, 50th, 75th and 90th) from before to during CRT, and after CRT ($p < 0.01$). There was no significant mean change in any K^{trans} quantiles ($p \geq 0.12$), skewness ($p \geq 0.10$) or kurtosis ($p \geq 0.06$) over time-points. There was a significant reduction in skewness in ADC histograms from before to after CRT ($p < 0.01$).

On analysis by time-point and response status (responder versus non-responder) (Table 2), the odds of being a responder was significantly higher for every unit increase in ADC 75th percentile value ($p = 0.049$) and ADC 90th percentile value ($p = 0.034$) after CRT (before surgery). The AUC for the 75th and 90th percentiles was 0.71 and 0.76, respectively, indicating acceptable discrimination. The mean whole tumour K^{trans} histogram quantiles were all higher before and during CRT, and lower after CRT in responders compared to non-responders, however there was no significant association with response status ($p > 0.10$). There was no significant association between ADC or K^{trans} skewness ($p \geq 0.16$ and $p \geq 0.22$, respectively) or kurtosis ($p \geq 0.51$ and $p \geq 0.47$, respectively) and response status at any time-point.

4. Discussion

This study investigated the use of DWI and DCE MRI in combination with a whole tumour heterogeneity analysis for the prediction of CRT response in patients with locally advanced rectal cancer. To the best of our knowledge, this is the first prospective study to incorporate a whole tumour heterogeneity assessment for both DWI and DCE-MRI. For the overall group, temporal changes in tumour heterogeneity were seen over the course of CRT; all ADC quantiles significantly increased over the time-points indicating reduced cellularity, ADC skewness significantly reduced from before to after CRT. After CRT (before surgery), the ADC 75th and 90th quantiles were found to be the most promising parameters for predicting response with higher ADC 75th and 90th quantile values significantly associated with responder status. K^{trans} quantile values were lower before and during CRT, and higher after CRT in non-responders compared with responders suggesting increased angiogenesis after CRT in non-responders, although this was not statistically significant.

This study demonstrated the benefit of considering measures other than the median to evaluate response and highlights the potential of intra-tumour heterogeneity analysis. There was no significant association of the median ADC with response outcome in this study. However, on analysis of whole tumour heterogeneity ADC histograms, ADC 75th and 90th percentiles after CRT (before surgery) were higher in the responder group than the non-responder group. The higher ADC 75th and 90th percentile values after CRT in responders were likely due to treatment-induced cell lysis and necrotic cells in the tumour bed resulting in presence of a fraction of cells in the tumour bed having very

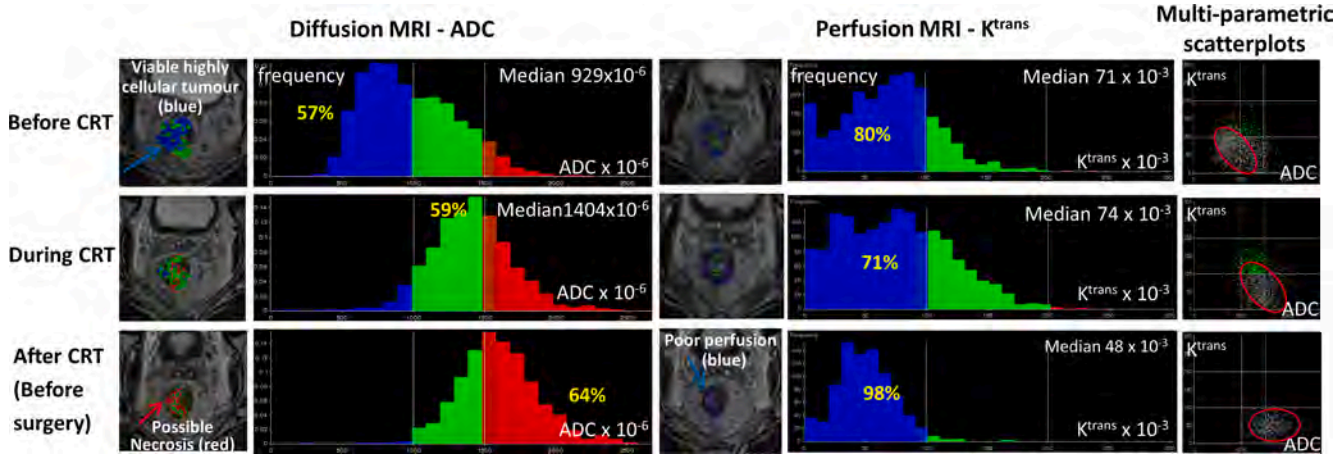

Fig. 2. Whole tumour ADC and K^{trans} color-coded maps, histograms, and multi-parametric scatterplots from OncoTreat for a responder (TRG 0, pathologic complete response). The ADC histograms demonstrated a shift in the distribution of ADC voxels to higher values, indicating reduced cellularity, over subsequent time-points. The K^{trans} histograms showed low K^{trans} values, indicating poor perfusion, and minimal change in K^{trans} over time-points. ADC histograms: blue voxels – ADC $< 1000 \times 10^{-6}$ mm^2/s, green voxels – ADC $1000–1500 \times 10^{-6}$ mm^2/s, red voxels – ADC $> 1500 \times 10^{-6}$ mm^2/s. K^{trans} histograms: blue voxels – K^{trans} values $< 100 \times 10^{-3}$mL/g/min, green voxels K^{trans} $100–200 \times 10^{-3}$ mL/g/min and red voxels $K^{trans} > 500 \times 10^{-3}$ mL/g/min. The percentage values indicate where the majority of voxel values lie. The multi-parametric scatterplots indicate the shift of ADC and K^{trans} values of voxels within the whole tumour over the time-points with the majority of voxels circled in red.

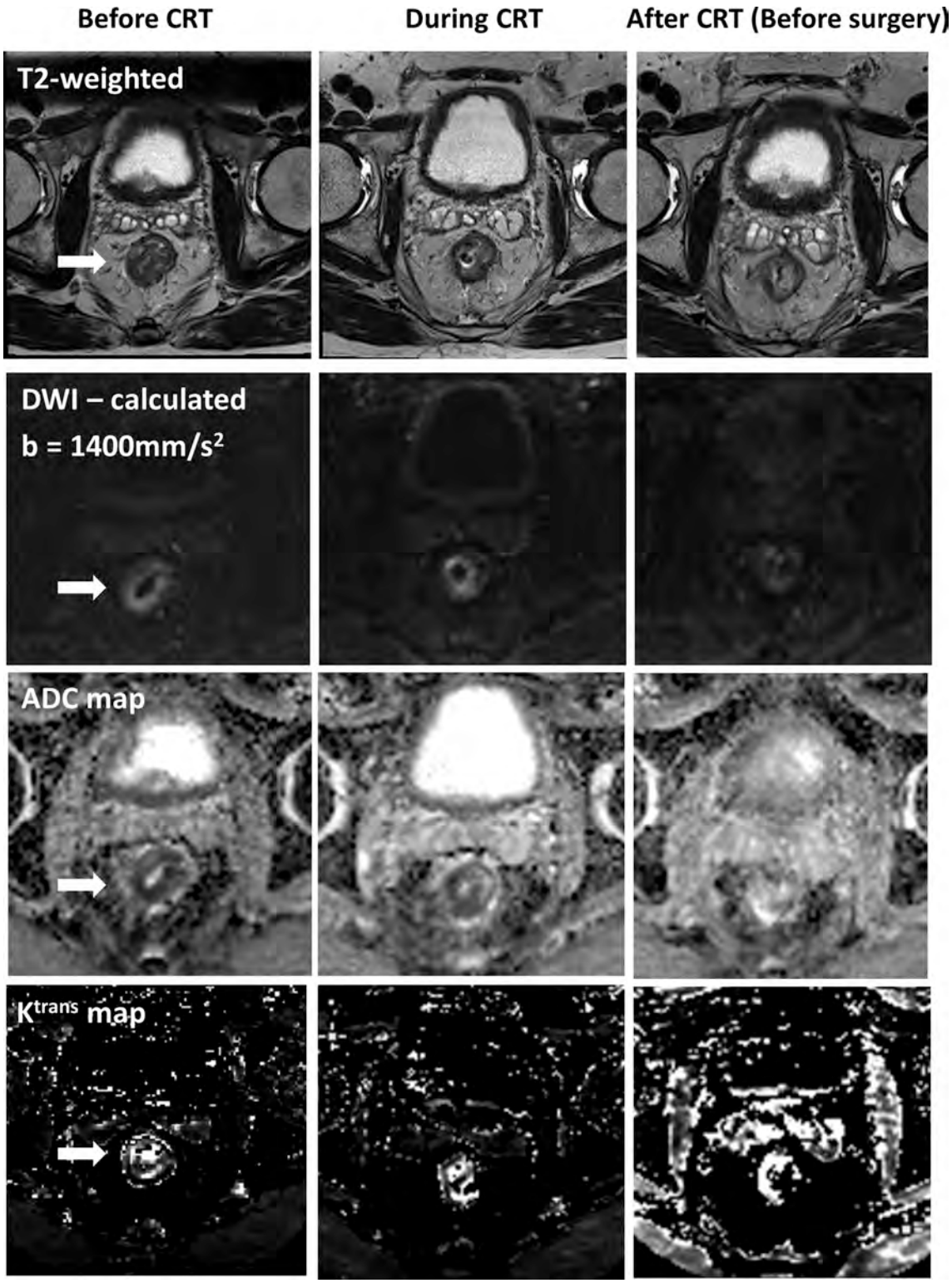

Fig. 3. Multi-parametric MRI at 3 time-points for a non-responder (TRG 2, minimal response). The arrow indicates the rectal tumour.

high ADC values in responders after CRT (before surgery). This study suggests that ADC 75th and 90th percentiles after CRT could be useful for selection of responders (TRG 0–1) for an organ preservation approach with either 'watch-and-wait' or local excision, thereby avoiding surgical morbidity such as permanent colostomy.

The DCE-MRI showed that non-responders had lower K^{trans} values before and during CRT, and higher K^{trans} values after CRT suggesting increased angiogenesis as a mechanism for therapeutic resistance. After CRT, the presence of high perfusion and K^{trans} in the tumour bed is suggestive of angiogenesis, persistent leaky vasculature and residual tumour. K^{trans} was not significantly associated with response however the study may have been underpowered due to small sample size. K^{trans} was selected for analysis in this study based on prior studies demonstrating K^{trans} to be promising in the prediction of CRT response [18,30], although there are no studies comparing which (semi)quantitative parameter is best for analysis. A systematic review by Dijkhoff et al. [31]

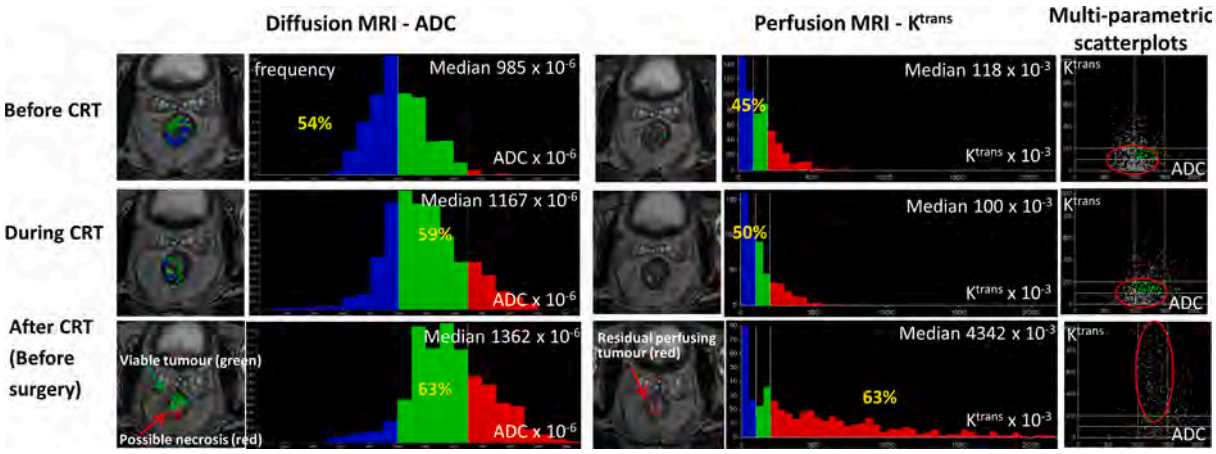

Fig. 4. Whole tumour ADC and K^{trans} color-coded maps, histograms and multi-parametric scatterplots from OncoTreat for a non-responder (TRG 2, minimal response). The ADC histograms showed a shift in ADC voxels to medium values in response to CRT. The K^{trans} histograms showed an increase in tumour perfusion after CRT. ADC histograms: blue voxels – ADC $< 1000 \times 10^{-6}$ mm^2/s, green voxels – ADC 1000–1500 $\times 10^{-6}$ mm^2/s, red voxels – ADC $> 1500 \times 10^{-6}$ mm^2/s. K^{trans} histograms: blue voxels – K^{trans} values $< 100 \times 10^{-3}$ mL/g/min, green voxels – K^{trans} 100–200 $\times 10^{-3}$ mL/g/min, red voxels – $K^{trans} > 500 \times 10^{-3}$ mL/g/min.

Table 1
Estimated change for all patients from baseline (95% CI) for a linear mixed-effects model of change over time for ADC and K^{trans} quantiles, skewness and kurtosis. P-values are from Dunnet multiple comparison with control (baseline value before CRT) test.

	ADC (x 10^{-6}): estimated change from before CRT to		K^{trans} (x 10^{-3}): estimated change from baseline to	
Histogram quantile/ statistic	During CRT (95%CI) p-value	After CRT (95%CI) p-value	During CRT (95%CI) p-value	After CRT (95%CI) p-value
10%	207 (145, 270) **p < 0.01**	299 (233, 364) **p < 0.01**	1.8 (−15.8, 19.3) p = 0.97	−6.1 (−24.1, 12.0) p = 0.68
25%	216 (163, 269) **p < 0.01**	326 (271, 382) **p < 0.01**	−4.9 (−49.9, 40.1) p = 0.96	−18.6 (−65.0, 27.7) p = 0.58
50%	213 (151, 275) **p < 0.01**	339 (274, 404) **p < 0.01**	10.1 (−78.9, 99.2) p = 0.96	−31.3 (−123.0, 60.4) p = 0.67
75%	203 (133, 272) **p < 0.01**	321 (248, 394) **p < 0.01**	91.0 (−86.4, 268.4) p = 0.42	−37.7 (−220.5, 145.0) p = 0.86
90%	195 (118, 272) **p < 0.01**	305 (225, 386) **p < 0.01**	223.0 (−71.4, 518.2) p = 0.17	−24.4 (−328.1, 279.3) p = 0.98
Skewness	−0.17 (−0.37, 0.03) p = 0.12	−0.29 (−0.50, −0.08) **p < 0.01**	−0.59 (−1.26, 0.08) p = 0.10	0.17 (−0.53, 0.87) p = 0.82
Kurtosis	−0.18 (−0.69, 0.34) p = 0.67	0.17 (−0.37, 0.70) p = 0.71	−11.72 (−23.83, 0.40) p = 0.06	−3.88 (−16.41, 8.65) p = 0.72

CRT: chemoradiotherapy, CI: confidence interval.

on DCE studies found that a higher K^{trans} before CRT in good responders to CRT was the most frequent finding. In DCE following CRT, a reduction of K^{trans} was found to be associated with good or complete response, and 2 studies found that K^{trans} after CRT was lower in good responders.

This study adds to the small number of published studies combining DWI and DCE-MRI for CRT response prediction in rectal cancer and adds to the validation of promising imaging biomarkers in rectal cancer [24,25,32], with the uniqueness of this study being the incorporation of whole tumour heterogeneity analysis for both DWI and DCE-MRI. Intven et al [24] assessed the combination of DWI and DCE-MRI at 2 time-points before CRT and after CRT for response assessment in rectal cancer in 55 patients and found that ADC was a promising tool for prediction of good response to CRT. However, the inclusion of K^{trans} did not increase the accuracy for response prediction. Our study similarly found that K^{trans} did not add any value in the prediction of CRT response.

A limitation in this study was the small number of patients particularly after CRT. There was considerable variability in histogram distributions. Multiple comparison adjustments were not employed. The findings require validation in a larger external cohort. Segmentations in this study were performed by a radiation oncologist with rectal cancer and MRI in radiotherapy expertise, and not a radiologist, which could be considered a limitation; however radiation oncologists have expertise in tumour delineation and are the likely clinicians to delineate MRI volumes for radiotherapy boosting. Scan reproducibility is a desirable characteristic to ensure stability of measured MRI biomarkers. The current dataset is undergoing further testing to assess the stability and reproducibility of MRI biomarkers across the different time-points.

The ability of MRI to map spatial and temporal functional heterogeneity in this study has future clinical utility in the targeting of tumour heterogeneity. MRI could be used to select patients with incomplete response, and spatial mapping of regions of incomplete response used to delineate the radiotherapy target for boosting with either photons (eg. MRI-Linac) or brachytherapy (contact X-rays, HDR endoluminal or interstitial brachytherapy), in order to increase the proportion of patients achieving a clinical complete response. Functional areas of persistent increased cellularity (low ADC) and perfusion (high K^{trans}) after CRT could be delineated for boosting.

This study used a simple manual two-parameter histogram analysis method in the MRI assessment of tumour heterogeneity that can be performed by the clinician. Radiomics is emerging as an alternative strategy to analyse MRI for response prediction that extracts information not visible to clinicians and this may improve response prediction. Radiomics is computational, high-throughput analysis of images that can extract thousands of parameters to characterise tumours. Nie et al used radiomics to extracted 103 imaging features, including histogram features, from baseline MRI (DWI and DCE) of 48 patients undergoing CRT in rectal cancer [33]. They found that a voxelised heterogeneity analysis had better prediction than a volume-averaged analysis. Bibault et al extracted 1683 radiomics features from 95 rectal cancer patients and created a deep neural network to that predicted pCR with 80% accuracy [34]. The challenges for the clinical translation of radiomics and deep learning models include complex computing workflows that are difficult to reproduce, low patient numbers for training and

Table 2
Unadjusted mean (SD) of ADC and K^{trans} quantiles, skewness and kurtosis by time and response status, odds ratio (odds of being a responder versus non-responder) and area under the curve (AUC) for patients with non-mucinous adenocarcinoma.

	Before CRT				During CRT				After CRT			
	Responder	Non-responder	Odds ratio (95% CI)	AUC (95% CI)	Responder	Non-responder	Odds ratio (95% CI)	AUC (95% CI)	Responder	Non-Responder	Odds ratio (95% CI)	AUC (95% CI)
	Mean (SD) of ADC (x 10^{-6})											
10%	652 (75)	690 (179)	1.00 (0.99, 1.00)	0.64 (0.44, 0.84)	879 (139)	878 (130)	1.00 (1.00, 1.01)	0.50 (0.28, 0.71)	970 (141)	975 (105)	1.00 (0.99, 1.01)	0.45 (0.22, 0.68)
25%	812 (94)	853 (153)	1.00 (0.99, 1.00)	0.60 (0.39, 0.80)	1050 (124)	1047 (122)	1.00 (0.99, 1.01)	0.50 (0.29, 0.72)	1186 (107)	1141 (79)	1.01 (1.00, 1.02)	0.43 (0.20, 0.67)
50%	1011 (125)	1039 (164)	1.00 (0.99, 1.00)	0.47 (0.26, 0.68)	1241 (125)	1234 (138)	1.00 (1.00, 1.01)	0.53 (0.32, 0.75)	1407 (137)	1327 (80)	1.01 (1.00, 1.02)	0.68 (0.45, 0.90)
75%	1252 (135)	1239 (173)	1.00 (1.00, 1.01)	0.54 (0.34, 0.75)	1459 (125)	1436 (156)	1.00 (1.00, 1.01)	0.55 (0.34, 0.77)	1626 (162)	1508 (101)	**1.01*** (1.001, 1.02)	**0.71** (0.50, 0.92)
90%	1496 (132)	1438 (191)	1.00 (1.00, 1.01)	0.60 (0.39, 0.80)	1686 (151)	1633 (172)	1.00 (1.00, 1.01)	0.59 (0.38, 0.80)	1844 (175)	1694 (128)	**1.01**** (1.001, 1.02)	**0.76** (0.57, 0.95)
Skewness	0.466 (0.552)	0.382 (0.404)	1.47 (0.34, 7.06)	0.54 (0.33, 0.75)	0.237 (0.396)	0.257 (0.500)	0.90 (0.17, 4.69)	0.50 (0.29, 0.72)	−0.015 (0.422)	0.240 (0.451)	0.22 (0.02, 1.44)	0.65 (0.43, 0.87)
Kurtosis	0.933 (1.007)	1.063 (0.916)	0.86 (0.39, 1.81)	0.59 (0.38, 0.79)	0.824 (0.521)	0.801 (0.773)	1.06 (0.34, 3.33)	0.50 (0.29, 0.72)	0.977 (0.781)	1.344 (1.844)	0.81 (0.36, 1.44)	0.52 (0.29, 0.75)
	Mean (SD) of K^{trans} ($\times 10^{-3}$)											
10%	36 (57)	27 (24)	1.01 (0.99, 1.03)	0.50 (0.28, 0.72)	36 (26)	30 (17)	1.01 (0.98, 1.05)	0.56 (0.34, 0.79)	18 (16)	31 (21)	0.96 (0.91, 1.01)	0.71 (0.49, 0.92)
25%	87 (169)	59 (50)	1.00 (1.00, 1.01)	0.53 (0.30, 0.76)	69 (42)	64 (32)	1.00 (0.98, 1.03)	0.48 (0.25, 0.70)	39 (33)	63 (48)	0.981 (0.96, 1.01)	0.67 (0.45, 0.89)
50%	152 (300)	117 (104)	1.00 (1.00, 1.01)	0.60 (0.38, 0.81)	152 (133)	135 (105)	1.00 (1.00, 1.01)	0.51 (0.28, 0.74)	74 (62)	123 (107)	0.99 (0.98, 1.00)	0.69 (0.47, 0.91)
75%	235 (473)	191 (196)	1.00 (1.00, 1.00)	0.63 (0.42, 0.85)	310 (363)	294 (342)	1.00 (1.00, 1.00)	0.57 (0.34, 0.79)	129 (124)	207 (203)	1.00 (0.99, 1.00)	0.72 (0.50, 0.94)
90%	321 (637)	270 (304)	1.00 (0.998, 1.002)	0.61 (0.39, 0.83)	526 (695)	508 (646)	1.00 (1.00, 1.00)	0.59 (0.36, 0.81)	208 (230)	316 (331)	1.00 (0.99, 1.00)	0.70 (0.46, 0.93)
Skewness	1.679 (1.625)	1.914 (1.668)	0.91 (0.51, 1.46)	0.58 (0.36, 0.80)	1.038 (0.584)	1.327 (0.633)	0.42 (0.09, 1.53)	0.65 (0.43, 0.86)	2.239 (1.776)	1.713 (1.196)	1.30 (0.74, 2.60)	0.58 (0.34,0.81)
Kurtosis	11.670 (26.040)	16.561 (37.801)	1.00 (0.96, 1.02)	0.60 (0.38, 0.82)	3.094 (5.311)	2.158 (3.774)	0.95 (0.75, 1.13)	0.59 (0.37, 0.81)	7.536 (10.412)	13.482 (27.160)	1.02 (0.97, 1.09)	0.61 (0.38, 0.84)

CRT: chemoradiotherapy; SD: standard deviation; CI: confidence interval; *p = 0.049, **p = 0.034 statistically significant.

validation sets, and need for clinical validation [35,36]. Radiomics and deep learning models that have been clinically validated in large patient datasets may be useful for response prediction and warrant further investigation.

In conclusion, DWI ADC and DCE K^{trans} histograms demonstrated intra-tumour heterogeneity in response to CRT. DWI-MRI ADC 75th and 90th quantiles after CRT were the most promising parameters for prediction of CRT responder status prior to surgery in patients with locally advanced rectal cancer. DCE-MRI K^{trans} did not add value in response prediction.

Declaration of Competing Interest

The authors declare that they have no known competing financial interests or personal relationships that could have appeared to influence the work reported in this paper.

Acknowledgements

This study was funded by the Royal Australian and New Zealand College of Radiologists (RANZCR) with a Withers and Peters $25000 competitive research grant. RANZCR was not involved in any aspect of the design, data collection, analysis, interpretation of data, writing of this study or decision to submit for publication. We would like to thank Dr Benjamin Schmitt and Siemens Healthineers for providing OncoTreat works-in-progress software.

Appendix A. Supplementary data

Supplementary data to this article can be found online at https://doi.org/10.1016/j.phro.2021.03.003.

References

[1] Kapiteijn E, Marijnen CAM, Nagtegaal ID, Putter H, Steup WH, Wiggers T, et al. Preoperative radiotherapy combined with total mesorectal excision for resectable rectal cancer. N Engl J Med 2001;345:638–46.

[2] Folkesson J, Birgisson H, Pahlman L, Cedermark B, Glimelius B, Gunnarsson U. Swedish rectal cancer trial: long lasting benefits from radiotherapy on survival and local recurrence rate. J Clin Oncol 2005;23:5644–50.
[3] Sauer R, Becker H, Hohenberger W, Rödel C, Wittekind C, Fietkau R, et al. Preoperative versus postoperative chemoradiotherapy for rectal cancer. N Engl J Med 2004;351:1731–40.
[4] Sauer R, Liersch T, Merkel S, Fietkau R, Hohenberger W, Hess C, et al. Preoperative versus postoperative chemoradiotherapy for locally advanced rectal cancer: results of the German CAO/ARO/AIO-94 randomized phase III trial after a median follow-up of 11 years. J Clin Oncol 2012;30:1926–33.
[5] Abraha I, Aristei C, Palumbo I, Lupattelli M, Trastulli S, Cirocchi R, et al. Preoperative radiotherapy and curative surgery for the management of localised rectal carcinoma. Cochrane Database Syst Rev 2018.
[6] Camma C, Giunta M, Fiorica F, Pagliaro L, Craxi A, Cottone M. Preoperative radiotherapy for resectable rectal cancer: a meta-analysis. JAMA 2000;284:1008–15.
[7] Maas M, Nelemans PJ, Valentini V, Das P, Rödel C, Kuo L-J, et al. Long-term outcome in patients with a pathological complete response after chemoradiation for rectal cancer: a pooled analysis of individual patient data. Lancet Oncol 2010;11:835–44.
[8] McCarthy K, Pearson K, Fulton R, Hewitt J. Pre-operative chemoradiation for non-metastatic locally advanced rectal cancer. Cochrane Database Syst Rev 2012;12.CD008368.
[9] Valentini V, Coco C, Cellini N, Picciocchi A, Fares MC, Rosetto ME, et al. Ten years of preoperative chemoradiation for extraperitoneal T3 rectal cancer: acute toxicity, tumor response, and sphincter preservation in three consecutive studies. Int J Radiat Oncol Biol Phys 2001;51:371–83.
[10] Valentini V, van Stiphout RGPM, Lammering G, Gambacorta MA, Barba MC, Bebenek M, et al. Nomograms for predicting local recurrence, distant metastases, and overall survival for patients with locally advanced rectal cancer on the basis of european randomized clinical trials. J Clin Oncol 2011;29:3163–72.
[11] Dhadda AS, Bessell EM, Scholefield J, Dickinson P, Zaitoun AM. Mandard tumour regression grade, perineural invasion, circumferential resection margin and post-chemoradiation nodal status strongly predict outcome in locally advanced rectal cancer treated with preoperative chemoradiotherapy. Clin Oncol 2014;26:197–202.
[12] van der Paardt MP, Zagers MB, Beets-Tan RGH, Stoker J, Bipat S. Patients who undergo preoperative chemoradiotherapy for locally advanced rectal cancer restaged by using diagnostic MR imaging: a systematic review and meta-analysis. Radiol 2013;269:101–12.
[13] Pham TT, Liney GP, Wong K, Barton MB. Functional MRI for quantitative treatment response prediction in locally advanced rectal cancer. Br J Radiol 2017;90.20151078.
[14] Barbaro B, Vitale R, Valentini V, Illuminati S, Vecchio FM, Rizzo G, et al. Diffusion-weighted magnetic resonance imaging in monitoring rectal cancer response to neoadjuvant chemoradiotherapy. Int J Radiat Oncol Biol Phys 2012;83:594–9.
[15] Lambrecht M, Vandecaveye V, De Keyzer F, Roels S, Penninckx F, Van Cutsem E, et al. Value of diffusion-weighted magnetic resonance imaging for prediction and early assessment of response to neoadjuvant radiochemotherapy in rectal cancer: preliminary results. Int J Radiat Oncol Biol Phys 2012;82:863–70.
[16] Monguzzi L, Ippolito D, Bernasconi DP, Trattenero C, Galimberti S, Sironi S. Locally advanced rectal cancer: value of ADC mapping in prediction of tumor response to radiochemotherapy. Eur J Radiol 2013;82:234–40.
[17] Patterson DM, Padhani AR, Collins DJ. Technology insight: water diffusion MRI–a potential new biomarker of response to cancer therapy. Nat Clin Pract Oncol 2008;5:220–33.
[18] George ML, Dzik-Jurasz ASK, Padhani AR, Brown G, Tait DM, Eccles SA, et al. Non-invasive methods of assessing angiogenesis and their value in predicting response to treatment in colorectal cancer. Br J Surg 2001;88:1628–36.
[19] de Vries A, Griebel J, Kremser C, Judmaier W, Gneiting T, Debbage P, et al. Monitoring of tumor microcirculation during fractionated radiation therapy in patients with rectal carcinoma: preliminary results and implications for therapy. Radiol 2000;217:385–91.
[20] de Lussanet QG, Backes WH, Griffioen AW, Padhani AR, Baeten CI, van Baardwijk A, et al. Dynamic contrast-enhanced magnetic resonance imaging of radiation therapy-induced microcirculation changes in rectal cancer. Int J Radiat Oncol Biol Phys 2005;63:1309–15.
[21] Yeo D-M, Oh SN, Jung C-K, Lee MA, Oh ST, Rha SE, et al. Correlation of dynamic contrast-enhanced MRI perfusion parameters with angiogenesis and biologic aggressiveness of rectal cancer: preliminary results. J Magn Reson Imaging 2015;41:474–80.
[22] Oberholzer K, Menig M, Pohlmann A, Junginger T, Heintz A, Kreft A, et al. Rectal cancer: assessment of response to neoadjuvant chemoradiation by dynamic contrast-enhanced MRI. J Magn Reson Imaging 2013;38:119–26.
[23] Just N. Improving tumour heterogeneity MRI assessment with histograms. Br J Cancer 2014;111:2205–13.
[24] Intven M, Monninkhof EM, Reerink O, Philippens MEP. Combined T2w volumetry, DW-MRI and DCE-MRI for response assessment after neo-adjuvant chemoradiation in locally advanced rectal cancer. Acta Oncol 2015;54:1729–36.
[25] DeVries AF, Kremser C, Hein PA, Griebel J, Krezcy A, Öfner D, et al. Tumor microcirculation and diffusion predict therapy outcome for primary rectal carcinoma. Int J Radiat Oncol Biol Phys 2003;56:958–65.
[26] Edge SBD, Compton C, Fritz A, Green F, Trotti A (Editors). AJCC Cancer Staging Manual. 7th ed.; 2012.
[27] Pham TT, Liney G, Wong K, Rai R, Lee M, Moses D, et al. Study protocol: multi-parametric magnetic resonance imaging for therapeutic response prediction in rectal cancer. BMC Cancer 2017;17.
[28] Royal College of Pathologists of Australasia (RCPA). Colorectal Cancer Structured Reporting Protocol. 2nd ed. Sydney: RCPA; 2012.
[29] Ryan R, Gibbons D, Hyland JMP, Treanor D, White A, Mulcahy HE, et al. Pathological response following long course neoadjuvant chemoradiotherapy for locally advanced rectal cancer. Histopathol 2005;47:141–6.
[30] Intven M, Reerink O, Philippens MEP. Dynamic contrast enhanced MR imaging for rectal cancer response assessment after neo-adjuvant chemoradiation. J Magn Reson Imaging 2015;41:1646–53.
[31] Dijkhoff RAP, Beets-Tan RGH, Lambregts DMJ, Beets GL, Maas M. Value of DCE-MRI for staging and response evaluation in rectal cancer: a systematic review. Eur J Radiol 2017;95:155–68.
[32] De Cecco CN, Ciolina M, Caruso D, Rengo M, Ganeshan B, Meinel FG, et al. Performance of diffusion-weighted imaging, perfusion imaging, and texture analysis in predicting tumoral response to neoadjuvant chemoradiotherapy in rectal cancer patients studied with 3T MR: initial experience. Abdom Radiol (NY) 2016;41:1728–35.
[33] Nie K, Shi L, Chen Q, Hu X, Jabbour SK, Yue N, et al. Rectal cancer: assessment of neoadjuvant chemoradiation outcome based on radiomics of multiparametric MRI. Clin Cancer Res 2016;22:5256–64.
[34] Bibault J-E, Giraud P, Housset M, Durdux C, Taieb J, Berger A, et al. Deep learning and Radiomics predict complete response after neo-adjuvant chemoradiation for locally advanced rectal cancer. Sci Rep 2018;8.
[35] Vallières M, Zwanenburg A, Badic B, Cheze Le Rest C, Visvikis D, Hatt M. Responsible radiomics research for faster clinical translation. J Nucl Med 2018;59:189–93.
[36] Kohoutová L, Heo J, Cha S, Lee S, Moon T, Wager TD, et al. Toward a unified framework for interpreting machine-learning models in neuroimaging. Nat Protoc 2020;15:1399–435.